Hybrid polymer matrix Terfenol-D composite / PMN-PT transducer in mechanical series configuration

Anthony P. Mortensen[a] and Marcelo J. Dapino[a]

[a] Department of Mechanical Engineering, The Ohio State University, Columbus, OH 43202

ABSTRACT

Combining smart materials with other materials to form composites has received attention due to the possibility of obtaining improved performance and functionality. One such composite combines Terfenol-D particulates with a soft epoxy, with the particles magnetically aligned in one direction forming an anisotropic structure. In this paper we consider the fabrication of the particle composites and the implementation of the composites in a hybrid ferroelectric/ferromagnetic transducer presented previously.[6] The composite was first tested quasistatically for obtaining material property information and identifying suitable bias conditions. The transducer was then tested for dynamic response, both of the individual parts and with the full system powered, for purposes of validating the concept of hybrid actuation and the model. The transducer is modeled through basic mechanical vibration principles, electroacoustics theory, and constitutive relations for electrostrictive and magnetostrictive materials operated in linear regimes. The paper highlights the advantageous properties of the Terfenol-D composite when utilized in this hybrid transducer in regard to the increased resistivity, decreased eddy current losses, and reduced density. The paper also proposes a model based approach for understanding the factors that control the reduced, and hence disadvantageous in some cases, stiffness and electromechanical coupling coefficient of the Terfenol-D composite.

Keywords: Terfenol-D, composites, PMN-PT electroacoustic theory, hybrid transducer

1. INTRODUCTION

In this paper we consider the transducer architecture shown in Fig. 1(a), which consists of a mechanical series arrangement of a terbium iron dysprosium (Terfenol-D) particle composite rod and a lead magnesium niobate-lead titanate (PMN-PT) stack, which are electrically connected in parallel. The mechanical series arrangement produces a double resonant design in which the lower and upper resonance are respectively controlled by the Terfenol-D and PMN-PT section, as represented by the lumped parameter system of Fig. 1(b). In this transducer, broadband response is possible due to the intrinsic ninety degree phase shift between magnetostrictive and piezoelectric velocities, and through the selection of appropriate design parameters as detailed previously.[2,3,6]

We consider a composite element consisting of Terfenol-D particles embedded in a vinyl ester resin as a replacement for the monolithic Terfenol-D rod employed in a previous Terfenol-D/PMN-PT device by Downey and Dapino.[6] The composite is expected to exhibit enhanced dynamic response due to reduced eddy current losses. Despite this critical advantage, a number of design and implementation issues arise due to the composite compliance, reduced electromechanical transduction, and reduced magnetoelastic properties. The paper is focused on the development of a system model based on that originally presented by Downey and Dapino,[6] aimed at analyzing the behavior of the new transducer and developing design criteria for achieving broadband transducer operation.

The model is motivated by both device design and material characterization, and comprises three main sets of equations: (i) mechanical vibrations equations for the transducer; (ii) equations for the individual active elements derived from classical electroacoustics theory which relate the applied voltages to the ensuing forces; and (iii) constitutive equations for the active elements which provide relationships between measured material properties and the electromechanical transduction coefficients developed in steps (i) and (ii). Combination of the three sets

Further author information: (Send correspondence to M.J.D.)
A.P.M.: Email: mortensen.19@osu.edu, Ph.: 614-247-7480
M.J.D.: Email: dapino.1@osu.edu, Ph.: 614-688-3689

Smart Structures and Materials 2005: Active Materials: Behavior and Mechanics,
edited by William D. Armstrong, Proceedings of SPIE Vol. 5761
(SPIE, Bellingham, WA, 2005) · 0277-786X/05/$15 · doi: 10.1117/12.600110

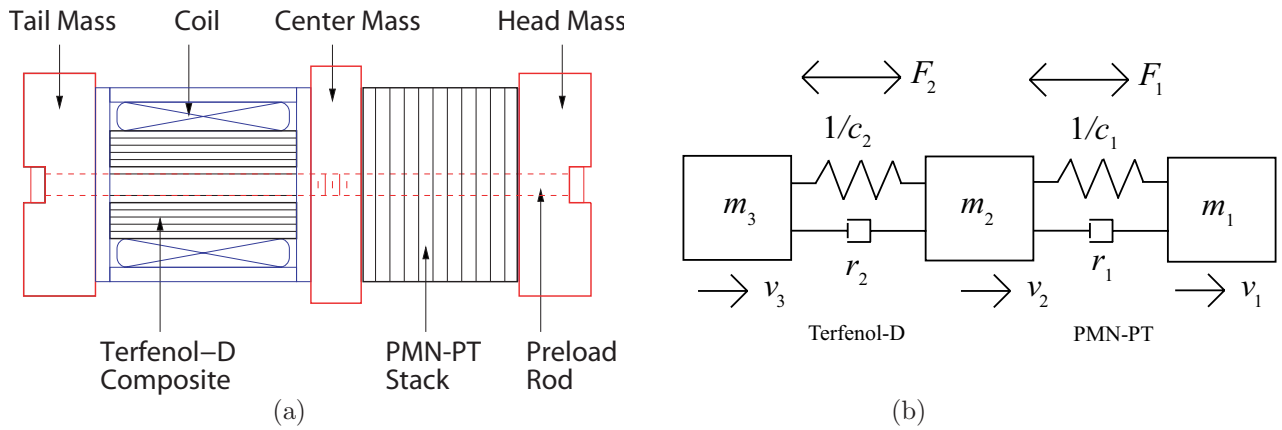

Figure 1. (a) Tonpilz-type hybrid ferroelectric/ferromagnetic transducer.[6] (b) Lumped-parameter vibratory model representing the hybrid transducer.

of equations expressed in the frequency domain yields expressions for the electrical impedance and head mass velocity. It is emphasized that both active elements are operated in biased, low signal regimes thus motivating the utilization of linear model equations. The model also permits extraction of material properties from dynamic impedance measurements, as opposed to the more conventional approach of extracting material properties from quasistatic strain and magnetization curves. The dynamic characterization approach is advantageous in that it yields material property information under conditions similar to those found in dynamic transducer operation.

The device presented by Downey and Dapino[6] can produce broadband head mass velocity response over the range from 500 Hz to 6 kHz. They also showed that by adding capacitance in series with the electrostrictive element, the electrical resonance frequency of the device can be tuned without fundamentally affecting its frequency bandwidth. This result has practical implications in that it allows matching of the transducer response to individual drivers. This could allow for retrofit of an existing hybrid device with a newer, more advanced ferroelectric stack without compromising the frequency bandwidth of the device. Earlier work by Butler and Tito[2] had demonstrated an underwater projector which follows the mechanical series arrangement of a magnetostrictive and a piezoelectric section originally proposed by Butler and Clark,[3] but in which the ratio of tail, center and head masses had been optimized for frequency bandwidth rather than unidirectional operation.

Terfenol-D produces large magnetostriction at room temperature with moderate fields but it does have some limiting issues. The material is very brittle which makes is susceptible to damage and difficult to machine. The material is solid and conductive which allows eddy currents to develop within the rod. This will result in energy loss that becomes more noticeable at higher frequency operations. Combining Terfenol-D with a binder can overcome most of these problems but at the cost of maximum magnetostriction and coupling coefficient. Experiments have been done with hard and soft binders. The stiffness of the binder restricts the strain. Hard binders are not capable of high strain. Soft binders are often used since they allow relatively high strain and insulate the particles to remove most energy loss from eddy currents. It also makes the material easy to machine and cast into many different shapes.

Magnetostrictive composites have been extensively investigated due to the various benefits that these materials offer relative to monolithic materials, especially concerning the reduced conductivity and associated reduction in eddy current losses and increase in frequency bandwidth. Composites with high volume fraction of Terfenol-D powder were extensively investigated in the 1990's with Sandlund et al. reporting results investigating 0-3 and 1-3 structure and volume fractions of over 70%.[19] The 0-3 isotropic structure is equivalent to randomly oriented and distributed particles thus approaching a constant stress condition. The 1-3 anisotropic architecture is achieved by aligning the particles in a magnetic field, which creates chains of Terfenol-D within the composite matrix and thus provides an approximately constant strain condition. Their tests suggest that in spite of a lower density, the composites with anisotropic structure exhibit improved magnetostriction and coupling factors over those with isotropic structure. The improvement in the anisotropic specimens is attributed

to the preferred crystal orientation of the particles along the easy axis. The tests also highlight the tradeoffs between high magnetostriction and decreased resistivity (which can limit the high-frequency performance) as the density of the composite is increased.

Low volume fraction 1-3 composites were investigated, for example, by Duenas and Carman.[10–12] By curing the composites at an elevated temperature, they were able to induce a mechanical prestress due to the difference in thermal expansions of the active and passive phase. Ruiz de Angulo[18] performed dynamic measurements to calculate the coupling coefficient and discovered a large reduction from the monolithic material which was later confirmed by Hudson.[14] This is not beneficial for actuator design but is very useful for damping applications as later investigated by McKnight and Carman.[17] Armstrong developed a model for composites that successfully model some of the nonlinear properties of the materials.[1]

The model considered in the paper for analysis and characterization of the hybrid transducer is discussed in Sec. 2. The experimental aspects of the work are presented in Sec. 3, while the measurements are discussed in Sec. 4. Finally, concluding remarks are presented in Sec. 5.

2. THEORY

2.1. Mechanical Model

The transducer behaves mechanically as a double resonant frequency response and is described by the three degree of freedom linear vibratory system shown in Fig. 1(b). Each active material is assumed to behave mechanically as a tunable compliance arranged in parallel with a damper. Here, m represents the mass, r the damping coefficient, c the mechanical compliance, v the velocity, F the force produced by the active elements in response to magnetic or electric fields, and s the Laplace derivative operator $j\omega$. The subscripts 1 and 2 on the applied forces, damping elements and compliances respectively denote the PMN-PT and Terfenol-D sections. The subscripts 1, 2, and 3 on the velocity vector respectively denote the head, center, and tail masses.

In order to determine criteria for broadband motion of the head mass, an expression for the mechanical impedance transfer function needs to be developed for each active section. To analyze the PMN-PT section, the force F_2 produced by the Terfenol-D composite rod is set equal to zero. The resulting impedance F_1/v_1 then takes the form[6]

$$Z_{mech,E} = \frac{F_1}{v_1} = \frac{As^4 + Bs^2 + C}{sc_1(m_2m_3c_2s^2 + (m_2 + m_3)(r_2c_2s + 1)}. \tag{1}$$

Proceeding in analogous fashion for the Terfenol-D rod one obtains

$$Z_{mech,M} = \frac{F_2}{v_1} = \frac{As^4 + Bs^2 + C}{sc_2m_3(r_1c_1s + 1)}. \tag{2}$$

The subscripts E and M respectively denote "electric" and "magnetic" for the PMN-PT and Terfenol-D elements. In equations (1)-(2), the terms A, B, and C have the form

$$\begin{aligned} A &= (m_1m_2m_3c_1c_2) \\ B &= m_3(m_1 + m_2)c_2(r_1c_1s + 1) + m_1(m_2 + m_3)c_1(r_2c_2s + 1) \\ C &= (r_1c_1s + 1)(r_2c_2s + 1)(m_1 + m_2 + m_3). \end{aligned}$$

Relations (1)-(2) are sufficiently general to characterize the transducer's output response due to activation of either smart material given suitable values for the material properties. Consistent with prior work,[2] Downey and Dapino[6] have determined that optimum bandwidth in this transducer is achieved using a head:center:tail mass ratio of approximately 1:2:2.5, and having the PMN-PT stack stiffness $1/c_1$ be much higher than that of the Terfenol-D rod, $1/c_2$. Using these mass values, the transducer output can be approximated by two dominant modes, the third being a zero-frequency rigid translation. The PMN-PT stack controls the upper resonance where the tail mass essentially decouples from the system and the head and center masses vibrate out of phase with each other. The lower resonance is controlled by the Terfenol-D section and is characterized by the head and center masses lumped together vibrating out of phase with the tail mass.

2.2. Electroacoustics Model

Classical electroacoustic transduction theory (Hunt, 1982) is now considered for purposes of coupling the vibratory model with the electrical regime. Considering the transduction model for general electromechanical transducers, two coupled relations can be written that describe the electrical and mechanical regimes. Assuming linearity, the expressions relating these two regimes are

$$V = Z_e I + T_{em} v \tag{3}$$

$$F = T_{me} I + Z_m v, \tag{4}$$

where V is the voltage across the transducer terminals, I is the current flow through the transducer, v is the velocity, F is the force, Z_e and Z_m respectively denote the blocked electrical and mechanical impedances, and T_{em} and T_{me} are coefficients that describe the electromechanical transduction. The subscripts *em* and *me* respectively denote "electrical due to mechanical" and "mechanical due to electrical" energy transduction processes. Certain properties of the electromechanical transduction process can be studied by considering the driving-point impedance at the electrical terminals, which is the complex ratio of voltage to current. For a general system described by the electroacoustic equations (3)-(4), it is assumed that the force F acts on a load of impedance Z_L, which allows (4) to be written in the form

$$v = \frac{-T_{me} I}{Z_m + Z_L}. \tag{5}$$

Substitution of this equation in (3) gives the total electrical impedance transfer function

$$Z_{ee} = \frac{V}{I} = Z_e + \frac{-T_{em} T_{me}}{Z_m + Z_L} = Z_e + Z_{mot}. \tag{6}$$

The total electrical impedance is composed of a blocked component Z_e equal to the ratio between voltage and current as the transducer is prevented to displace, and a motional component Z_{mot} associated with the mechanical motion of the transducer and load. The motional component provides a measure of the amount of electromechanical coupling in the transducer.

The electrical resonance frequency f_r is determined from the principal diameter of the Nyquist representation of the electrical impedance transfer function.[6] The electrical impedance function and its inverse, the admittance function $Y_{ee} = 1/Z_{ee}$, provide *different* measures of transducer figures of merit such as coupling coefficients, quality factors, elastic moduli, and sound speeds.[5, 8, 15] Indeed, although the total impedance and admittance functions are the inverse of one another, the coupled motional effects are not, i.e., $Y_{mot} \neq 1/Z_{mot}$. One difference between these functions is that in the admittance loop the frequency opposite the crossover point is the antiresonance frequency f_{ar} rather than f_r. As detailed for Terfenol-D by Dapino et al.,[5] the resonant and antiresonant frequencies quantify the effective coupling coefficient through the relations

$$k_{eff}^2 = \begin{cases} 1 - \left(\frac{f_{ar}}{f_r}\right)^2, & \text{if } f_{ar} < f_r \\ 1 - \left(\frac{f_r}{f_{ar}}\right)^2, & \text{if } f_{ar} > f_r \end{cases} \tag{7}$$

which respectively apply to PMN-PT and Terfenol-D. In conjunction with the system masses, the resonance and antiresonance frequencies offer a means of calculating the stiffness of each drive element. The stiffness is determined by setting the imaginary component equal to zero in expressions (1) and (2) and rearranging

$$k_m^E = \frac{1}{c_1} = \frac{(2\pi f_r)^2 m_1 m_2}{m_1 + m_2},$$

$$k_m^M = \frac{1}{c_2} = \frac{(2\pi f_r)^2 (m_1 + m_2) m_3}{m_1 + m_2 + m_3}.$$

Here, the superscripts E and M respectively denote the PMN-PT (electric field) and Terfenol-D (magnetic field) sections. Assuming linearly elastic behavior, the Young's moduli of the PMN-PT and Terfenol-D drivers are respectively given by

$$E_y^E = \frac{k_m^E L_{e,1}}{A_1}$$
$$E_y^M = \frac{k_m^M L_{e,2}}{A_2},$$

where L_e and A (with appropriate subindices) denote length and cross sectional area of each active element.

The electrical impedance and admittance measurements allow the direct determination of the mechanical quality factor of each section,

$$Q_r = \frac{f_r}{f_2 - f_1} \tag{8}$$

$$Q_{ar} = \frac{f_{ar}}{f_{a2} - f_{a1}}. \tag{9}$$

Since each section has two values for Q, the average value is used for transducer design and model validation. By inspection of the mechanical equations of motion, the internal damping is estimated by

$$r_1 = \frac{2\pi f_r m_1 m_2}{Q(m_1 + m_2)} \tag{10}$$

$$r_2 = \frac{2\pi f_r (m_1 + m_2) m_3}{Q(m_1 + m_2 + m_3)} \tag{11}$$

respectively for the PMN-PT and Terfenol-D sections. The above equations relating experimental measurements to transducer figures of merit were employed in this study to determine the model parameters for each section.

2.3. Constitutive Electroacoustic Relations

The electroacoustic relations developed in Sec. 2.2 provide a framework which is sufficiently general to analyze a variety of electromechanical systems. However, in these relations no distinction has been made between ferroelectric and ferromagnetic behavior, which is particularly distinct in terms of the phase between velocity and applied voltage. To address this limitation, the electroacoustic relations (3)-(4) are combined with constitutive equations which describe the strain and polarization produced by the active materials. This will allow for the blocked impedances and transduction coefficients to be expressed in terms of material properties and design parameters for each section.

2.3.1. Terfenol-D Section

Assuming biased operation about low field inputs, we first consider linear piezomagnetic constitutive relations for a Terfenol-D rod driven along the longitudinal "33" direction,

$$\varepsilon = \frac{\sigma}{E_y^M} + qH \tag{12}$$

$$B = q^*\sigma + \mu^\sigma H, \tag{13}$$

where ε is the strain, σ is the axial stress, H is the magnetic field, B is the magnetic flux density, μ^σ is the permeability at constant stress, and $q = q^*$ is a symmetric magnetoelastic coupling coefficient. To convert these expressions into a form compatible with relations (3) and (4), the following electromechanical relations

are employed

$$H = nI$$
$$\varepsilon = \frac{v}{j\omega L_{e,2}}$$
$$\sigma = \frac{F}{A_2}$$
$$V = RI + j\omega NBA_2,$$

where n is the turns ratio of the magnetic coil ($n = N/L_{e,2}$), $L_{e,2}$ is the length of the coil and composite rod, A_2 is the rod cross sectional area and internal area of the coil, and R is the wire resistance. The total voltage drop is that of a DC resistance R in series with an electrical inductance. Substitution of these expressions into (12) and (13), and subsequent rearrangement yields[13]

$$V = [R + j\omega\mu^{\sigma}(1 - k_{eff}^2)n^2 A_2 L_{e,2}]\, I + Nqk_m^M\, v, \tag{14}$$

$$F = -Nqk_m^M\, I + \frac{k_m^M}{j\omega}\, v. \tag{15}$$

Comparison of these equations with the general electroacoustic relations (3)-(4) gives

$$Z_{e,M} = R + j\omega\mu^{\sigma}(1 - k_{eff}^2)n^2 A_2 L_{e,2} = R + j\omega L_{block}, \tag{16}$$

where L_{block} is defined as $\mu^{\sigma}(1 - k_{eff}^2)n^2 A_2 L_{e,2}$. This indicates that the blocked electrical impedance $Z_{e,M}$ for the Terfenol-D section can be represented by an ideal resistor in series with an inductor L_{block} which can be directly determined from measured material properties.

Equations (14) and (15) also determine the transduction coefficients T_{em} and T_{me}. These terms describe the coupling between the electrical and mechanical regimes and can be related to material properties by

$$T_{em,M} = Nqk_m^M \tag{17}$$

$$T_{me,M} = -Nqk_m^M = -T_{em,M}. \tag{18}$$

It is observed that $T_{em,M}$ and $T_{me,M}$ are equal in magnitude while opposite in sign, as is expected of all magnetostrictive transducers because of the spatial orthogonality of current and magnetic field.[15]

2.3.2. PMN-PT Section

For low field inputs about a bias field or for materials which exhibit quasilinear behavior, as is the case when this particular PMN-PT stack is operated at room temperature, the constitutive behavior of individual layers can be approximated by the linear piezoelectric constitutive relations, which in strain-charge form are given by

$$\varepsilon = \frac{\sigma}{E_y^E} + dE \tag{19}$$

$$D = d^*\sigma + \epsilon^{\sigma}E, \tag{20}$$

where E is the electric field, D is the electric charge density, E_y^E is the Young's modulus at constant field, ϵ^{σ} is the electric permittivity at constant stress, and $d = d^*$ is a symmetric electroelastic coupling coefficient. Relationships analogous to those derived for magnetostrictive materials have the form

$$E = \frac{V}{t}$$
$$\varepsilon = \frac{v}{j\omega L_{e,1}}$$
$$\sigma = \frac{F}{A_1}$$
$$D = \frac{I}{j\omega A_1},$$

in which it is assumed that each layer has thickness t and cross-sectional area A_1. Substitution of these expressions into (19) and (20), followed by suitable rearrangement yields

$$V = \frac{t}{A_1 j\omega N(\epsilon^\sigma - E_y^E d^2)}\, I + \frac{-dE_y^E}{j\omega N(\epsilon^\sigma - E_y^E d^2)}\, v \tag{21}$$

$$F = \frac{-dE_y^E}{j\omega N(\epsilon^\sigma - E_y^E d^2)}\, I + \frac{\epsilon^\sigma E_y^E A_1}{j\omega N(\epsilon^\sigma - E_y^E d^2)}\, v. \tag{22}$$

Comparison of these relations with the general electroacoustic relations (3)-(4) indicates that the blocked electrical impedance of the PMN-PT stack is purely capacitive,

$$Z_{e,E} = \frac{t}{j\omega A_1 N(\epsilon^\sigma - E_y^E d^2)} = \frac{1}{j\omega C_{block}}, \tag{23}$$

where $C_{block} \equiv A_1 N(\epsilon^\sigma - E_y^E d^2)/t$. The two coefficients that characterize the electromechanical transduction can be written from equations (21) and (22) as

$$T_{em,E} = \frac{-dE_y^E}{j\omega N(\epsilon^\sigma - E_y^E d^2)} \tag{24}$$

$$T_{me,E} = \frac{-dE_y^E}{j\omega N(\epsilon^\sigma - E_y^E d^2)}. \tag{25}$$

Consistent with the electrical nature of ferroelectric transduction, and in contrast with the Terfenol-D section, the coefficients are symmetric since they are identical in both magnitude and sign. It was mentioned that the velocities of the two sections are ninety degrees out of phase, and that this property is useful in extending bandwidth.[2] This inherent phase shift can be proven by comparing the transduction coefficients T_{em} of each section as shown by Downey and Dapino.[8]

2.4. Combined Linear Transducer Model

With all of the electroacoustic coefficients defined in terms of physical parameters, relations (14)-(15) and (21)-(22) are used to calculate the velocity response to an applied input voltage. It is noted that the relationship between applied voltage and velocity is determined by the coefficients $T_{em,M}$ and $T_{em,E}$.

Since the PMN-PT and Terfenol-D sections are wired in electrical parallel, their total electrical impedances including motional contributions sum as normal. Thus the transducer's total electrical impedance, incorporating electrical and mechanical effects in both active sections, is

$$Z_{ee,total} = \frac{Z_{ee,E}\, Z_{ee,M}}{Z_{ee,E} + Z_{ee,M}}, \tag{26}$$

in which $Z_{ee,M}$ is quantified by (6), (16), (17) and (18), and $Z_{ee,E}$ by (6), (23), (24) and (25).

To quantify the head mass velocity response, first the current in each section is found from the definition of electrical impedance,

$$I_E = \frac{V}{Z_{ee,E}}$$

$$I_M = \frac{V}{Z_{ee,M}}$$

where the applied voltage is V for both sections. The velocity contribution from each section is given by (5),

$$v_E = \frac{-T_{me,E}\, I_E}{Z_{m,E} + Z_L}$$

$$v_M = \frac{-T_{me,M}\, I_M}{Z_{m,M} + Z_L}.$$

The final step in the velocity calculations is to recognize that the mechanical series configuration allows for the superposition of the velocities from the two sections, which results in

$$v = v_E + v_M. \tag{27}$$

This also allows for the comparison of the individual section responses by graphing just $Z_{ee,E}$ and v_E or $Z_{ee,M}$ and v_M. Each set assumes no electrical input and thus no excitation of the other section but does account for the coupling due to the attached mechanical components.

3. EXPERIMENTAL SETUP

3.1. Transducer design

The original hybrid transducer was designed and constructed to use an ETREMA Terfenol-d rod ($Tb_{0.73}$ $Dy_{0.27}$ $Fe_{1.95}$) with a length of 50.8 mm (2 in) and a diameter of 6.35 mm (0.25 in).[7] The field is created by a 1200 turn coil consisting of 26-AWG magnet wire with a single-layer pick-up coil on the inside diameter. The magnetic coil is enclosed in an Alnico V permanent magnet which creates a dc magnetic field of 125 Oe (10 kA/m) and is axially slit to reduce eddy currents. The magnetic circuit is completed with machined 1018 steel components. The rod is positioned between the 777 g tail mass and the 670 g center mass as seen in Fig. 2. Each mass is 76.2 mm (3 in) diameter and made from non magnetic stainless steel. Three bolts hold the rod between the masses with belleville washers placed under the bolt heads to provide the preload necessary for optimal Terfenol-D performance. The electrostrictive component of the transducer is composed of an EDO Ceramic model EP200-62 EC-98 stack. The material is lead magnesium niobate - lead titanate in a 65-35 ratio which has a quasi-linear response at room temperature. This ceramic was selected for its stiffness of approximately 120×10^6 N/m to create the two mechanical resonances desired when placed in series with the magnetostrictive section. The stack is composed of 62 individual layers and has a total length of 35.2 mm (1.385 in) and a diameter of 16 mm (0.63 in). The stack is placed between the center mass and the 308 g head mass with three bolts used to hold the masses together and belleville washers to provide the necessary preload to maintain the stack in compression. The finished transducer has a length of 152.4 mm (6 in). Although the transducer was designed for operating with monolithic Terfenol-D rod, we replaced the rod with a composite sample of the same dimensions. Due to the reduced stiffness of the composite, Belleville washers were added in series with the preload springs to reduce the mechanical bias.

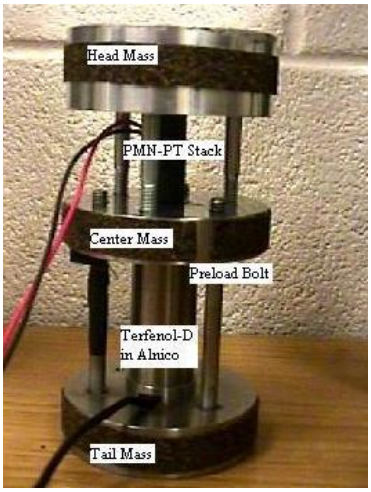

Figure 2: Fully assembled hybrid transducer

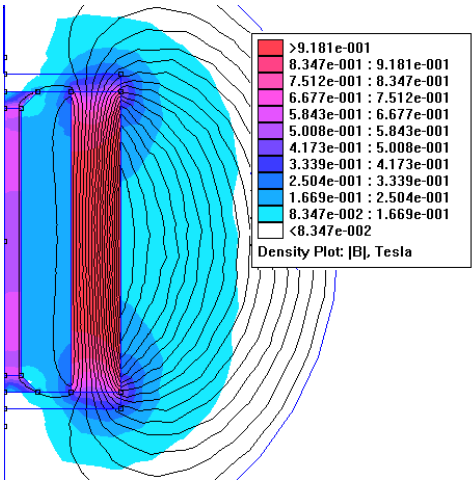

Figure 3: FEA model of mold and magnetic circuit

3.2. Composite Design and Fabrication

The desired specimen size for the testing equipment is a 2" (50.8 mm) long rod with a diameter of 1/4" (6.35 mm). To achieve higher magnetostriction, the particles must be aligned with a magnetic field. The resulting chains of particles in the matrix create an anisotropic structure which is often referred to as a (1-3) structure, as opposed to the isotropic (0-3) structure. The test specimens are magnetized along the cylinder axis to align the particles. It is desirable that the field used to align the particles is homogeneous throughout the sample to adequate ideal particle distribution. If the field is too low in the middle, the particles may not align with the axis, while a high concentration of magnetic field at the rod ends may pull the particles to the poles. Finite element modeling was utilized to design a mold with a magnetic circuit that would achieve even distribution as seen in Fig. 3. End magnets were found to not provide a uniform field, so a permanent magnet in the shape of a hollow cylinder was selected, see Fig. 4(a)-(b). A semi continuous magnetic circuit was designed to effectively balance the field throughout the specimen. This was achieved by using steel end caps smaller than the magnet, thus creating a gap which increases the magnetic reluctance in the right amount. The end caps are tapered to aid the magnetic flow while the gap between the steel parts and magnet prevents the ends of the mold from becoming magnetized in excess, thus pulling the particles toward the ends.

The samples were made from a low viscosity resin that hardens at room temperature when combined with a catalyst and promoter. The resin takes a yellow color when it dries but is not noticeable in the Terfenol-D samples. Low viscosity resin permits more effective wetting of the particles which decreases the void content of the material caused by small gas pockets clinging to the particles. The Terfenol-D ball-milled powder was supplied by ETREMA Products, Inc. The particle size ranged from 106 to 300 microns which is the larger size range available. This was selected since previous research demonstrated that very small particles exhibit less strain.[12] The samples were mixed in an open air environment and no degassing was performed. This is unusual for magnetostrictive composites but it has been demonstrated that preparing samples in an argon environment and repeated degassing can have little to no effect on the composite performance,[9] while greatly increasing the complexity of the manufacturing process. The mold was sealed with silicone to prevent the epoxy from leaking out. The magnet was slipped over the mold as soon as the epoxy was poured. A guide was used to slide the magnet over the mold quickly so the particles would not separate. All the samples were cured in an oven to ensure complete reaction of the epoxy and catalyst, and later machined on a lathe to obtain flat ends.

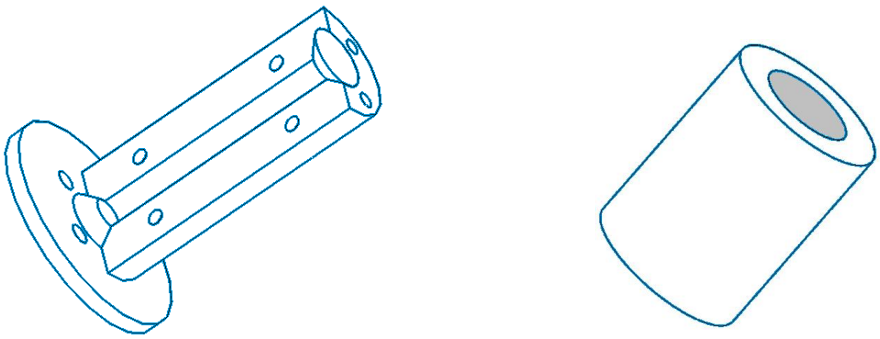

(a) (b)

Figure 4. (a) A two-part aluminum mold surrounds the sample with a steel end cap at either end and an aluminum plate to hold the end caps and magnet in place when fully assembled. (b) Neodymium iron boron (NdFeB) hollow cylindrical magnet poled along the axis and sized to slip over the mold.

4. MEASUREMENTS

Quasistatic time domain tests were performed on the Terfenol-D composite rod and PMN-PT stack to determine the properties q, μ^{σ}, and d for the characteristic equations. The bias points were selected from theses tests to find a steep linear region. Fig. 5(a)-(b)s show major loop tests for the strain and magnetization of the composite rod compared with those of monolithic Terfenol-D. In the dynamic tests, a bias field of 4.7 kOe (381 kA/m)

was employed in combination with an ac field of the same 0-pk magnitude. It is observed in Fig. 5(a)-(b) that these field values are excessive as the resulting response is located past the steepest region or "burst" zone.

Dynamic experiments were conducted with the transducer suspended by a string to isolate the system and prevent exogenous dynamics from affecting the transducer. Low frequency tests were conducted independently for the Terfenol-D composite and the PMN-PT stack to determine the quasi-static linear coupling coefficients q and d. The composite was tested in a water cooled transducer[16] to measure strain vs field "butterfly" curve with the motion measured by a linear variable differential transducer (LVDT). The magnetic bias and AC drive level were selected to limit motion to the steepest region on the curve. Broadband tests were conducted using a sine sweep function from 100 Hz to 6 kHz. The measured quantities include the acceleration of the head mass, applied voltage and applied current. The dynamic tests were conducted with each section driven independently and with the two sections wired in parallel. The composite was tested with a constant preload and varying AC field or DC bias to characterize the material dynamically. Acceleration tests were also performed for varying preload with constant bias and field.

A constant DC bias of 63 kA/m was used at various fixed AC fields from 3.1–37.6 kA/m, as shown in Fig. 6. Increasing the magnetic field decreases the resonance frequency and causes the material to become more compliant. This is more noticeable at higher fields. Higher fields also increase the magnitude of the impedance curve but also appears to dampen out the impedance. In related tests shown in Fig. 7, a constant AC field of 12.5 kA/m was used for various fixed bias fields. Although the resonance frequency does not change as the bias is varied, the magnitude response does increase with increasing field. Additional dynamic measurements were conducted with a 63 kA/m DC field and a 12.5 kA/m AC field, with the electrostrictive section left as an open circuit. The free floating acceleration test with only the Terfenol-D section active exhibit resonance frequencies that increase with increasing mechanical preload, as shown in Fig. 8. This trend is also noticeable when the preload is increased with the full transducer active, as shown in Fig. 9. The lower resonance frequency increases with mechanical preload and has negligible effect on the higher resonance which is dominated by the electrostrictive element. There is an anti resonance around 2000 Hz which may be caused by a vibration absorber effect created by the mechanical system since the transducer was originally designed to work with monolithic Terfenol-D. The added damping of the composite also changes the phase difference between the materials which when reduced to 0 (or 180) degrees would cause a large antiresonance.

The transducer electrical impedance was measured from the voltage and current monitors on the amplifiers. A sine sweep was used to excite the transducer and tests were run for both the electrostrictive and magnetostrictive section powered with the other element left as an open circuit. The entire transducer was powered

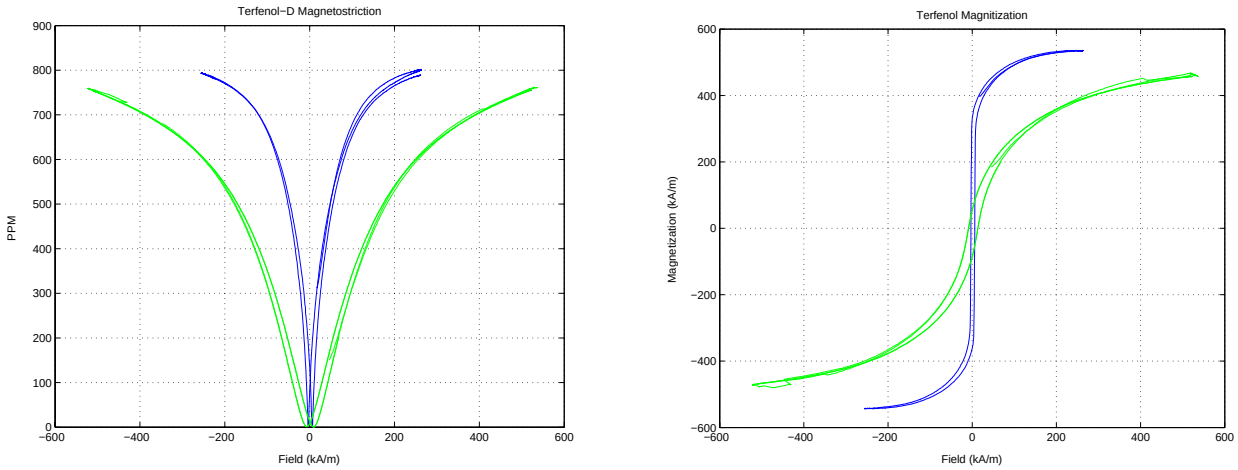

(a) (b)

Figure 5. (a) Quasistatic strain as a function of magnetic field for a 50 percent volume fraction composite sample (wider curve) and a monolithic piece of Terfenol-D. (b) Corresponding magnetization measurements.

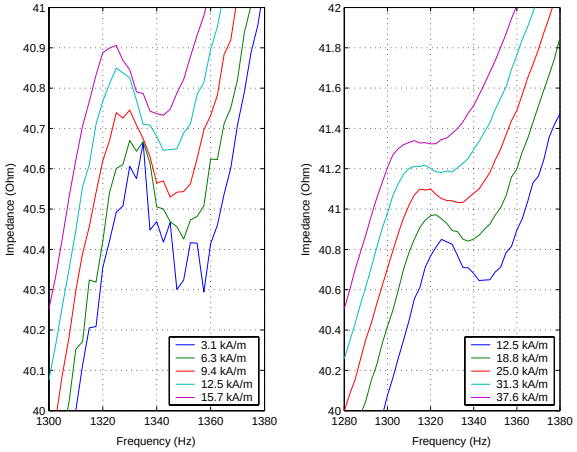

Figure 6. Electrical impedance at constant magnetic bias of 63 kA/m with varying AC magnetic field.

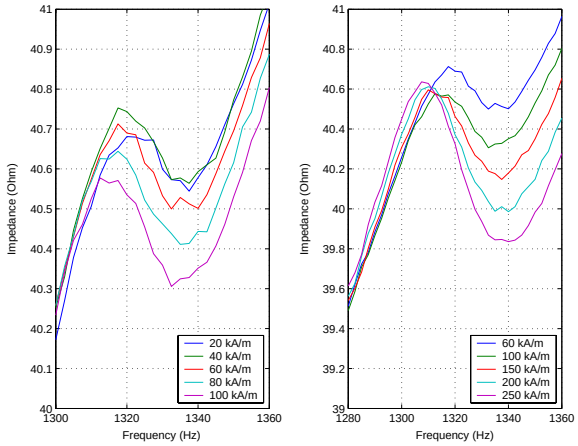

Figure 7. Electrical impedance at constant AC magnetic field of 12.5 kA/m with varying DC magnetic bias.

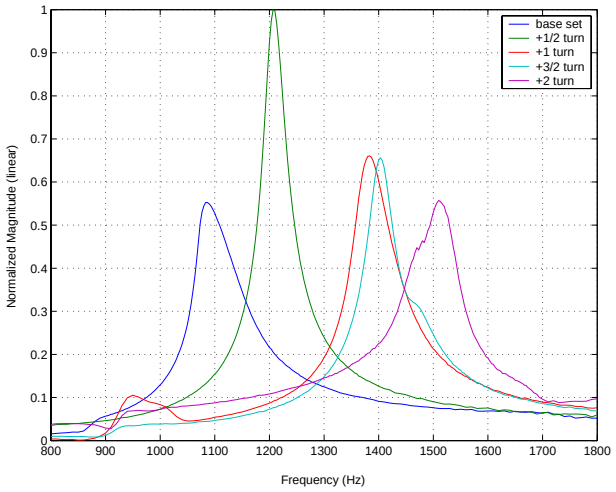

Figure 8. Acceleration vs current with transducer ends unrestrained, Terfenol-D composite active only.

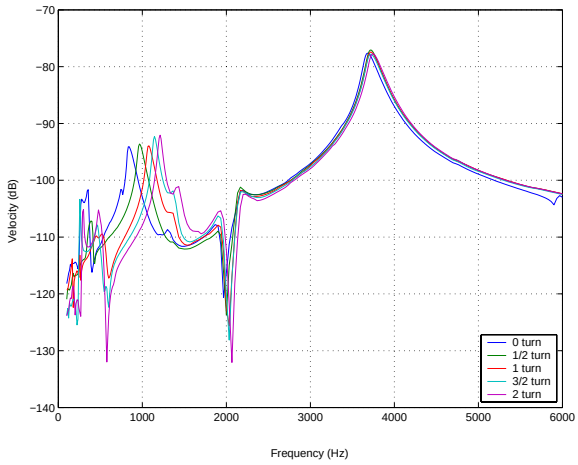

Figure 9. Full transducer acceleration with varying mechanical loads on the composite element.

with both elements wired in electrical parallel. The electrical impedance measurements show a double resonance for the system, one corresponding to the PMN-PT stack and the other to the overall electrical resonance.T he loop associated with the Terfenol-D composite is too small to be observed due to the reduced electromechanical transduction coefficient of this particular composite sample.

5. CONCLUDING REMARKS

Hybrid ferroic transducers are capable of extending performance over single element devices due to their complementary electromechanical properties. In the case of PMN-PT and Terfenol-D, the phase shift between the materials helps to create extended bandwidth. Terfenol-D can be combined with other materials to create composites that can exhibit better high-frequency response while being machinable. However, these improvements come at the expense of increased compliance and reduced electromechanical transduction. On the other hand, the low density of the composites considered here can yield improved weight energy densities. Further work will be performed to investigate and understand the factors that control these performance tradeoffs in hybrid

transducers. This understanding will be used to implement the models discussed in this paper for the hybrid transducer employing the Terfenol-D composite and PMN-PT.

REFERENCES

1. W.D. Armstrong, "Nonlinear behavior of magnetostrictive particle actuated composite materials," *Journal of Applied Physics,* 87(6):3027–3031", 2000.
2. S.C. Butler and F.A. Tito, "A broadband hybrid magnetostricitive/piezoelectric transducer array," *OCEANS MTS/IEEE*, 3:1469-1475, 2000.
3. J.L. Butler and A.E. Clark, "Hybrid piezoelectric and magnetostrictive acoustic wave transducer," US Patent No. 4,443,731, 1984.
4. Y. Chen, J.E. Snyder, C.R. Schwichtenberg, K.W. Dennis, and D.K. Falzgraf, "Effect of elastic modulus of the matrix on magnetostrictive strain in composites," *App. Phys. Letters,* 74(8):1159–1161, 1999.
5. M.J. Dapino, A.B. Flatau, and F.T. Calkins, "Statistical anaysis of Terfenol-D material properties," *Journal of Intelligent Material Systems and Structures,* in review.
6. P.R. Downey and M.J. Dapino, "Extended frequency bandwidth and electrical resonance tuning in hybrid Terfenol-D/PMN-PT transducers in mechanical series configuration," *Journal of Intelligent Material Systems and Structures,* in print.
7. P.R Downey, "Hybrid PMN-PT/Terfenol-D broadband trnaducers in mechanical series configuration," Masters Thesis, The Ohio State University, 2003.
8. P.R. Downey, M.J. Dapino, and R.C. Smith, "Analysis of hybrid PMN/Terfenol broadband transducers in mecahnical series configuration," *Proceedings of SPIE Smart Structures and Materials,* 5049:168–179, 2003.
9. T.A. Duenas and G.P. Carman, "Particle distribution study for low-volume fraction magnetostrictive composites," *Journal of Applied Physics*, 90:2433–2439, 2001.
10. T.A. Duenas and G.P. Carman, "Large magnetostrictive response of Terfenol-D resin composites," *Journal of Applied Physics,* 87:4696–4701, 2000.
11. T.A. Duenas and G.P. Carman, "Experimental results for magnetostrictive composites, Proceedings of ASME/IMECE, Adaptive Structures and Material Systems Symposium, 63-71, 1998.
12. T.A. Duenas, L. Hsu and G.P. Carman, "Magnetostrictive composite material systems analytical/experimental," *MRS Proceedings: Advances in Smart Materials*, 1996.
13. D. Hall, "Dynamics and vibrations of magnetostrictice transduers," Ph.D. Dissertation, Iowa State University, 1994.
14. J. Hudson, S.C. Busbridge and A.R. Piercy, "Magnetomechanical coupling and elastic moduli of polymer-bonded Terfenol composites," *Journal of Applied Physics*, 83(11):7255-7257, 1998.
15. F.V. Hunt, "Electroacoustics: The analysis of transduction, and its historical background," American Institute of Physics for the Acoustical Society of America, 1982.
16. A. Malla, "Effect of composition on the magnetic and elastic properties of shape memory Ni-Mn-Ga," Masters Thesis, The Ohio State University, 2003.
17. G.P. McKnight and G.P. Carman, "Energy Absorption and damping in magnetostrictive composites," *Materials Research Society Proceedings, Adaptive Structures and Material Systems,* 604:267-272, 2000.
18. L. Ruiz de Angulo, J.S. Abell, and I.R. Harris, "Magnetostrictive properties of polymer bonded Terfenol-D," *Journal of Magnetism and Magnetic Materials,* 157-158, 1996.
19. L. Sandlund, M. Fahlander, T. Cedell, A.E. Clark, J.B. Restorff, and M. Wun-Fogle, "Magnetostriction, elastic moduli, and coupling factors of composite Terfenol-D," *Journal of Applied Physics*, 75:5656-5658, 1994.